Design of All-fiber Coupled Electro-optic Sensors for High Power Microwave

Lili Song, Juntao He, Junpu Ling, Tao Jiang, and Danni Zhu
College of Optoelectronic Science and Engineering
National University of Defense Technology, Changsha, Hunan 410073, China

Abstract— A novel design of all-fiber coupled Electro-Optic (EO) sensors is introduced. Special fiber apparatus is used instead of free-space-coupling using bulk optics such as conventional lenses. The reflectance dependence on some parameters of the sensor is analyzed, such as the incident angle, the thickness of the crystal, the space between collimator and crystal, the under tested E-field, etc.. According to the analysis, the exact thickness of the $LiTaO_3$ crystal is calculated when attached to the collimator, which can make the reflectance and sensitivity to maximum.

1. INTRODUCTION

In the 1980s, A. Yariv gives the formula of the EO tensor coefficients. Since then, EO sensing technology has gained considerable attention due to its lower destruction [1], higher resolution [2] and broader frequency band [3] in both near-field and far-field in microwave measurement. Comparing to antenna based sensors, EO sensors present a flat response over a much broader frequency bandwidth (~ 8 decades) [2], a much higher spatial resolution on the order of the size of the laser-beam diameter or even less [4], and much less interference to the field under tested as no metal is used. Additionally, measurement in the terahertz (THz) region can be achieved when the thickness of EO crystal is on the order of $1 \sim 10\,\mu\text{m}$ and the optic source is ultra-short pulse laser [4–6]. Moreover, EO sensors are independent of the mode of the microwave while antenna based sensors can only be available to special modes as the distribution of the antenna array is restricted.

Most researchers use polarizer, Wollaston prism, half-wave plates or quarter-wave plates for E-field measurement [1–7], which needs complex modulation and is immovable. Besides, the working condition is rigorous. Hence, building a sensing system with stable performance and straightforward operation is essential. This paper will show an all-fiber coupled EO sensing system which will make up these disadvantages aforementioned.

It's apparent that the design and optimization of EO sensors are crucial to achieving high-quality microwave sensing. Different sensitivities can be achieved with different structures and the enhancement of the interaction length of the crystal can improve the sensitivity [5, 8]. Fabry-Perot (F-P) cavity is efficient to improve the sensitivity, fortunately, without reduction of the spatial resolution as the volume of the crystal does not increase [5, 8, 9]. This paper displays detailed analysis and design progress of an F-P cavity based EO sensor with the application of $LiTaO_3$ crystal.

2. DESIGN OF ALL FIBER-COUPLED EO SENSOR SYSTEM

Instead of lens and plates, a polarization maintaining optical circulator (PMOC) and a polarization beam splitter (PBS) are used. The experimental schematic is composed of a laser, a PMOC, a PBS, an EO sensor and two photodiodes as shown in Figure 1. The laser comes out through Port ii (reflective port) after getting through the PMOC from Port i (import), and then sends to the EO crystal. The beam is reflected to Port ii by the crystal, then comes out from Port iii (export) and arrives at the PBS. The laser will be divided into 2 parts of different polarizations by the splitter, the ordinary beam and the extraordinary beam, detected by two photodiodes PD1 and PD2.

The thickness of the crystal in use should be negligible comparing to the wavelength of the E-field under tested, while it should be much larger than the wavelength of the detective laser. Figure 2 is a schematic of EO sensor whose structure is similar to an F-P cavity as the adjacent areas in both sides of the crystal are air. The EO sensor is composed of polarization maintaining fiber, a collimator (1/4 GRIN Lens), EO crystal and glass ferrule that makes the structure stable. The quasi F-P cavity configuration has drawn a lot of attention because of the following benefits. Firstly, the sensitivity is higher thanks to the enhancement of interference components [5, 8]. What's more, the Signal-to-Noise Ratio is larger [9]. Next, we take such a quasi F-P cavity structure into consideration.

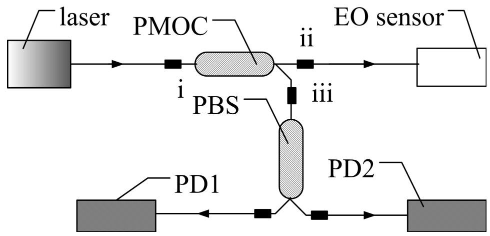

Figure 1: Schematic of all fiber-coupled EO probing system.

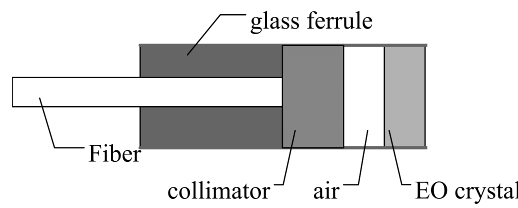

Figure 2: Schematic of EO sensor.

Suppose that the wavelength of the detective laser is λ, the thickness of the crystal is h, the thickness of the air layer between the collimator and the crystal is d, and n_o and n_e are the refractive indexes of the ordinary beam and the extraordinary beam of the crystal in the absence of E-filed, respectively. r_{13} and r_{33} are EO coefficients, E_z is the Z-component of the E-field under tested, δ_0 and δ_e are the phase retardations of the ordinary beam and the extraordinary beam in the appearance of E-field, respectively. The reflected beam of the F-P cavity can be expressed as in Figure 3. If $\theta_1 = 0$, we get the reflectance as Equation (1).

$$\begin{aligned} r &= \sum_{n=1}^{\infty} r_n = \frac{r_1 + r_2 e^{i\delta}}{1 + r_1 r_2 e^{i\delta}} \\ R &= r \cdot r^* = \frac{r_1^2 + r_2^2 + 2r_1 r_2 \cos\delta}{1 + r_1^2 r_2^2 + 2r_1 r_2 \cos\delta} \end{aligned} \tag{1}$$

where r is the amplitude reflectance and R is the reflectance of the detective laser.

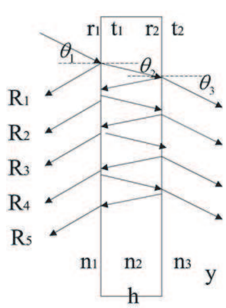

Figure 3: Schematic of reflected light in F-P cavity.

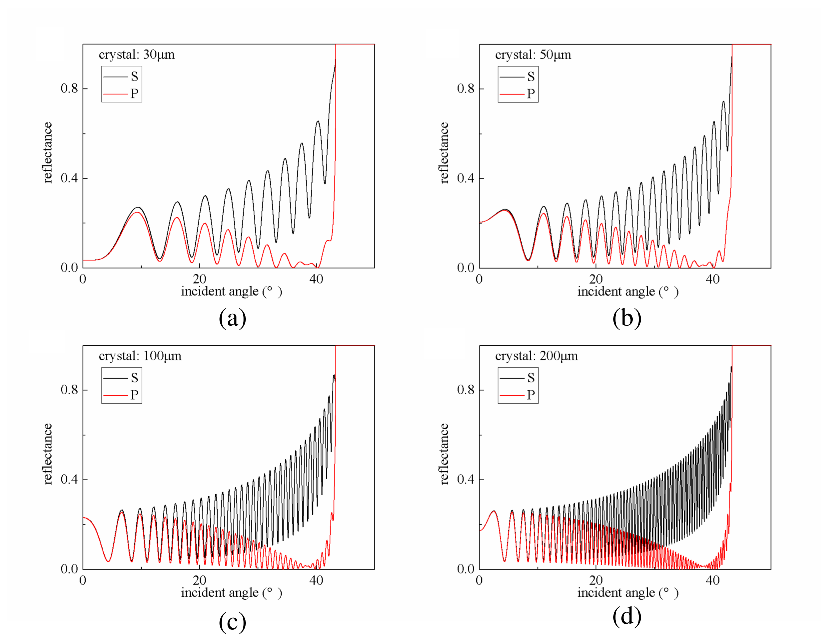

Figure 4: Reflectance dependence on incident angles with different thicknesses of crystal while $d = 0$.

3. ANALYSIS OF THE ALL FIBER-COUPLED EO SENSOR

To choose a suitable laser wavelength λ (incident wavelength), the optical communication window $\lambda = 1550$ nm is taken into consideration, where the attenuation is rather small. The principles of choosing the EO crystal are as following. Firstly, from Equation (1), it is obvious that the response of E_z is in proportion to either r_{13} or r_{33}. Therefore, the EO coefficients of the crystal should be large enough in the purpose of achieving higher sensitivity. Secondly, the absorption of the crystal to the detective laser beam should be small enough. In addition, the crystal should be with low temperature effect, high optical damage threshold, good optical uniformity as well as easy to manufacture. In general, the available crystals series are mainly 3 m, 4 mm, 6 mm, 6 m^{-2} and 4 m^{-3}. We choose $LiTaO_3$ for analysis as r_{13} and r_{33} can get to 6.95×10^{-12} m/V and 27.4×10^{-12} m/V [10] respectively at $\lambda = 1550$ nm. Besides, the optical damage threshold reaches 1550 GW/m^2 [11]. The refractive indexes of the crystal are $n_o = 2.1186$ and $n_e = 2.1224$. Furthermore, $n_1 = 1.457$ and $n_3 = 1$, representing refractive indexes of fiber and the air, respectively [10].

3.1. Reflectance Dependence on the Incident Angle of the Laser

In general, the dominate parameters affecting the reflectance are the incident angle, the thickness of the crystal h, the space between collimator and crystal d, the under tested E-field, etc.. First, the relationship between the incident angle and reflectance is analyzed in Figure 4. For simplification, only the extraordinary beam is considered, which can be realized when the fiber is coupled to the ordinary axis, and the thickness of the air between the collimator and the crystal d is assumed to be 0. The thickness of the EO crystal h is set at four different values, 30 µm, 50 µm, 100 µm, and 200 µm, to simulate the relationship between the reflective efficiency and the incident angle of the laser ranging from 0° to 50°, as is shown in Figures 4(a)–(d). Black curves are the reflectance of the S-polarized beam and red curves are the reflectance of the P-polarized beam.

According to Figure 4, reflectance of the S-polarized beam fluctuates in localities and the maximum values rise overall. Reflectance of the P-polarized beam fluctuates in localities and the maximum values decrease at first and then increase. For all the curves, reflectance approaches 100% when the incident angle is close to 43.34° as a result of total reflectance, while the numerical value solved with the Refractive Law is 43.3385°. When the thickness of the crystal become thicker as shown in Figures 4(a) to (d), the curves fluctuate in a shorter period, which is due to the F-P effect. When the optical length of the incident wave induced by the crystal is the even multiples of half wavelength, a reflective beam in a given order is enhanced by the one in the next order, As a result, reflectance reaches maximum values in several incident angles. The minimum values appear when the optical length of the incident wave induced by the crystal is the odd multiples of half wavelength.

3.2. Reflectance Dependence on the Thickness of Crystal

The next analyzed parameter in this study is the thickness of crystal h. Figure 5 shows the reflectance dependence on the thickness of the crystal at normal incidence. The thickness of the air layer between collimator and crystal d is assumed to be 0. From the figure we can see the curves vary owing to the F-P effect. The following paragraph will give a more detailed explanation of this phenomenon. To get a maximum value, $R' = 0$, $R'' \leqslant 0$, that is,

$$R'(h) = 8\pi n/\lambda \frac{r_1 r_2(1-r_1^2)(1-r_2^2)\sin\delta}{(1+r_1^2 r_2^2+2r_1^2 r_2^2\cos\delta)^2} = 0 \tag{2}$$

$$R''(h) = 32\pi^2 n^2/\lambda^2 \frac{r_1 r_2(1-r_1^2)(1-r_2^2)}{(1+r_1^2 r_2^2+2r_1^2 r_2^2\cos\delta)^3}(2\sin^2\delta+\cos\delta+\cos\delta r_1^2 r_1^2+2r_1 r_2\cos^2\delta) \leq 0 \tag{3}$$

To satisfy these two conditions, we can get Equation (4),

$$n_0 h/\lambda = \frac{k_1}{2}, \quad k_1 = 1, 2, 3, \ldots \tag{4}$$

Equation (4) is in consistent with Figure 5. Sensitivity can be maximized in the condition of $R'' = 0$, then we can get Equation (7),

$$n_0 h/\lambda = \frac{1}{4\pi} ar\cos\left(\frac{(1+r_1^2 r_2^2)\pm\sqrt{r_1^4 r_2^4+2r_1^2 r_2^2-8r_1 r_2+9}}{4(1-r_1 r_2)}\right)+\frac{k_2}{2}, \quad k_2 = 1, 2, 3, \ldots \tag{5}$$

According to Equation (4) and Equation (5), suitable thickness of the crystal can be chosen to realize high quality measurement, and the reflectance can reach the maximal values when $h = 365.807k_1$ (µm), $k_1 = 1, 2, 3, \ldots$ when the crystal is attached to the collimator. The sensitivity can be maximized when $h = 0.1227 + 0.3658k_2$ (µm), $k_2 = 1, 2, 3, \ldots$ in the same structure.

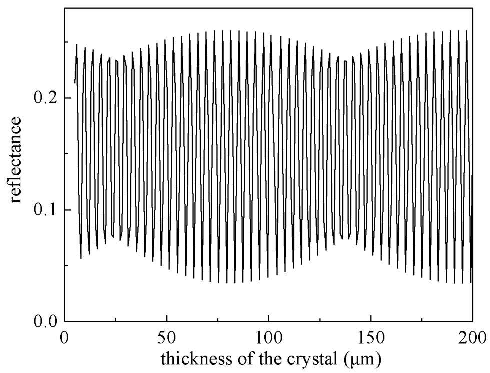

Figure 5: Reflectance dependence on the thickness of crystal at normal incidence.

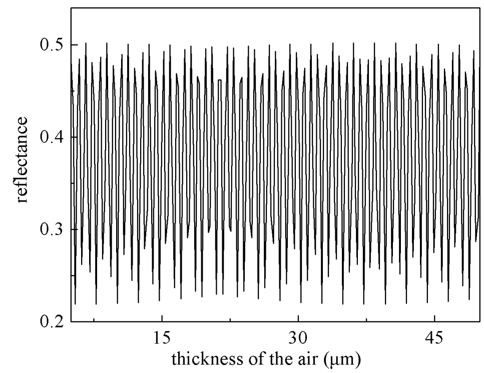

Figure 6: Reflectance dependence on d at normal incidence with $h = 100\,\mu\text{m}$.

3.3. Reflectance Dependence on the Space between the Crystal and the Collimator

The reflectance dependence on the thickness of the air layer between the collimator and the crystal d is similar to that on the thickness of the EO crystal h as both are correlative to the optical length. Figure 6 is the reflectance dependence on the thickness of the air layer between collimator and the crystal at normal incidence with $h = 100\,\mu\text{m}$. The reflectance increases comparing to Figure 5 in the appearance of the air between the collimator and the crystal.

3.4. Reflectance Dependence on *E*-field under Test

Figure 7 shows the reflectance dependence on E_z under tested with $h = 200\,\mu\text{m}$ and $d = 0$. The maximum E_z is 100 MV/m in Figure 7(a) while 1 MV/m in Figure 7(b) as the damage level of the EO sensor is known to be in the order of 1 MV/m [13]. The red curves and black curves are the reflectance of the ordinary beam and the extraordinary beam, respectively.

According to Figure 7(a), the extraordinary beam has a higher sensitivity to E_z as the EO coefficient r_{33} is almost four times of r_{13}. In Figure 7(b), no repeated value occurs of the either the ordinary beam or the extraordinary beam when the E-field is smaller than 1 MV/m, which makes the operation easier in practical measurement.

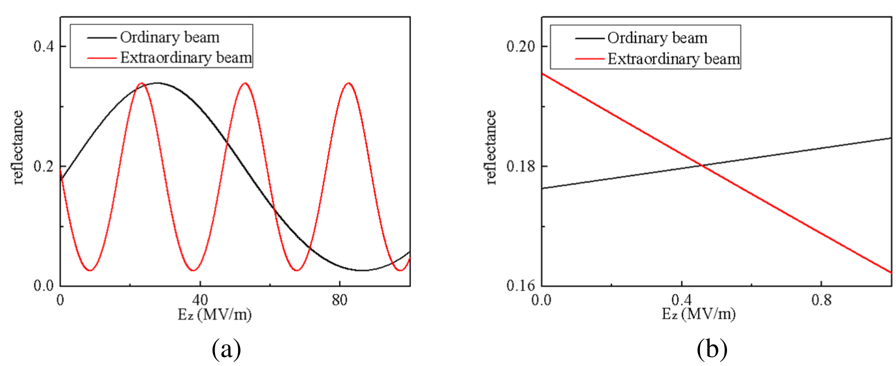

Figure 7: Reflectance dependence on E_Z of ordinary beam (red) and extraordinary (black) beam in FAC structure.

4. CONCLUSION

We introduced a novel all-fiber coupled EO sensor, and analyzed the parameters which may influence the reflectance, such as the incident angle, the thickness of the crystal, the thickness of the air layer between the collimator and the crystal and the E-field under test. Based on the analysis using $LiTaO_3$ as the EO crystal, total reflectance appears when the incident angle is close to 43.34°. Reflectance increases in the appearance of the air between the collimator and the EO crystal. Reflectance can get the maximum value when $h = 365.807k_1$ (μm), $k_1 = 1, 2, 3, \ldots$ when the crystal is attached to the collimator. The sensitivity can be maximum when $h = 0.1227 + 0.3658k_2$ (μm), $k_2 = 1, 2, 3, \ldots$ in the same structure.

REFERENCES

1. Bernier, M., L. Duvillaret, and G. Gaborit, "Fully-automated *E*-field measurement system using pigtailed electro-optic sensors for temperature-dependent-free measurements of microwave signals in outdoor conditions," *IEEE*, Vol. 9, No. 1, 61–68, 2008.
2. Bnoek, E., D. Hornbachner, E. R. Bratengeyer, et al., "Electro-optic elf field sensor," 1992.
3. Quang, D. L., D. Erasme, and B. Huyart, "Fabry-perot enhance real-time electro-optic probing of MMICs," *Elec. Lett.*, Vol. 29, No. 5, 498–499, 1993.
4. Yang, K., G. David, S. V. Robertson, et al., "Electrooptic mapping of near-field distributions in integrated microwave circuits," *IEEE*, Vol. 46, 1998.
5. Mitofanov, O., "Terahertz near-field electro-optic based on a microresonator," *Appl. Phys. Lett.*, Vol. 88, 2006.
6. Bakker, H. J., G. C. Cho, and H. Kurz, "Distortion of terahertz pulses in electro-optic sampling," *Opt. Soc. Am. B*, Vol. 15, 1795–1801, 1998.
7. Duvillaret, L., S. Rialland, and J. L. Coutaz, "Electro-optic sensors for electric field measurements. II. Choice of the crystals and complete optimization of their orientation," *J. Opt. Soc. Am. B,* Vol. 19, 2704–2715, 2002.
8. Lee, D. J., N. W. Kang, and J. H. Choi, "Recent advances in the design of electro-optic sensors for minimally destructive microwave field probing," *Sensors*, Vol. 11, 806–824, 2011.
9. Muller, P. O., S. B. Alleston, and A. J. Vickers, "An external electro-optic sampling technique based on the Fabry-Perot effect," *IEEE J. Quantum Electron*, Vol. 35, 7–11, 1999.
10. Zeng, W., D. P. Wang, and Y. H. Xu, "Growth and photoreflective resistance properties of near-stoichiometric Zn: LiTaO3 crystal," *Journal of Chinese Ceramic Society*, Vol. 37, No. 11, 1829–1832, 2009.
11. Yariv, A. and P. Yeh, *Optical Waves in Crystals*, Science Press, Beijing, 1991.
12. Garzarella, A., S. B. Qadri, and D. H. Wu, "Optimal electro-optic sensor configuration for phase noise limited, remote field sensing applications," *Appl, Phys. Lett.*, Vol. 94, 1–3, 2009.